



OPEN

Unusual behaviour of the spin-phonon coupling in the quasi-one-dimensional antiferromagnet RbCoCl_3

M. G. Cottam¹✉ & D. J. Lockwood²

We present an experimental and theoretical study for the lattice vibrational (phonon) modes in the quasi-one-dimensional (or chain-like) antiferromagnet RbCoCl_3 at low temperatures both above and below the two different magnetic phase transitions. Clear evidence is found for the role of spin-phonon interactions in providing a temperature-dependent contribution for the frequencies of the E_{1g} and E_{2g} symmetry phonons that occur with frequencies comparable to those of the spin wave excitations (magnons) in this compound. The behaviour in RbCoCl_3 , as studied here by Raman scattering experiments, is quite different from that typically observed in rutile-structure antiferromagnets where the spin-phonon coupling has been well characterized. The theory is modified to take account of the strong Ising-like component in the spin Hamiltonian. This enables the spin-phonon coupling parameters to be deduced, with the analysis also revealing the onset of an extra frequency shift for the phonons below the transition temperature $T_{N1} = 28$ K associated with magnetic ordering along the Co chains.

Spin-phonon coupling in magnetic solids is ubiquitous¹ and is important for many of the physical properties of such solids. The signature of the sometimes strong, but usually subtle, interaction between lattice vibrational modes (phonons) and spin waves (magnons) in the magnetically ordered state can take various forms that are often best studied at near-zero wave vector, which makes them ideal for optical investigations using inelastic light scattering (Raman or Brillouin spectroscopy)¹ or infrared absorption. A thorough knowledge of such spin-phonon coupling is very important for understanding the full physical properties in the dynamics of magnetic materials and can be the determining factor for the applications of certain materials in practical applications²⁻⁴.

There has been sustained interest in recent years regarding the novel properties of hexagonal perovskite compounds of the form ABX_3 , where A is Cs, Rb or Tl, B is a divalent metal ion, and X is an alkali halide (typically Cl or Br). The hexagonal crystal structure is as shown in outline in Fig. 1, where the positions of the magnetic B atoms (Co in this case) have been emphasized. Such perovskites containing spin-1/2 magnetic Co ions have been found to exhibit quasi one-dimensional (1D) antiferromagnetic ordering at low temperatures as a result of dominant Ising model exchange interactions occurring along the chains of Co magnetic ions (see Fig. 1). Features of interest include spin-wave energy continua and the possibility of bound magnon states and their potential applications in spin-1/2 quantum-wire transport devices. Rubidium cobalt chloride (RbCoCl_3) is an example of such a desirable magnetic material, because of its classic quasi 1D magnetic ordering^{5,6}, and will be studied here for that reason. Most of these transition metal perovskites exhibit two magnetic phase transitions at temperatures denoted by T_{N1} and T_{N2} , respectively. The higher of these transition temperatures, T_{N1} , represents the temperature below which there is antiferromagnetic ordering in one dimension along the chains, whereas the lower temperature T_{N2} signifies the onset of an additional 3D inter-chain ordering due to exchange interactions between Co ions within crystalline a - b planes (see Fig. 1). A large amount of neutron scattering work, as well as optical measurements such as Raman scattering and far infrared spectroscopy, for these compounds have been used to determine their structural and dynamic properties. These experimental studies have included CsCoCl_3 (see, e.g.⁷⁻¹¹), RbCoCl_3 ¹²⁻¹⁵, TlCoCl_3 ¹⁶, and CsCoBr_3 ^{8-10,17-19}.

It has been shown from symmetry considerations that, given the D_{6h} hexagonal symmetry of the crystalline unit cell, the Raman active phonons at zero wave vector in RbCoCl_3 comprise the A_{1g} , E_{1g} and three E_{2g} modes¹³. Symmetry coordinates for all 30 different vibrational modes at zero wave vector in crystals with the

¹Department of Physics and Astronomy, University of Western Ontario, London, ON N6A 3K7, Canada. ²Metrology Research Centre, National Research Council, Ottawa, ON K1A 0R6, Canada. ✉email: cottam@uwo.ca

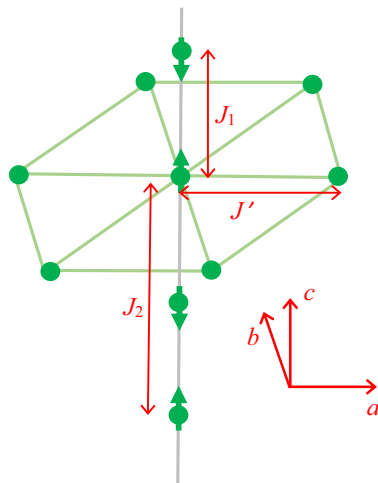


Figure 1. Schematic of crystal structure of RbCoCl_3 , showing the Co ions only (filled green circles) ordered antiferromagnetically along chains (in the crystallographic c direction) with nearest-neighbour exchange J_1 and next nearest-neighbour exchange J_2 . Each Co ion is surrounded by a hexagon of six Co ions with interchain exchange interaction J' in the a - b plane.

same structure as RbCoCl_3 have been determined²⁰. Polarized Raman scattering has been used to identify the various phonons, and at ~ 11 K their frequencies are 60.6 (E_{2g} mode), ~ 115 (E_{1g}), 132.1 (E_{2g}), 192.9 (E_{2g}), and 272.6 (A_{1g}) cm^{-1} ¹³.

Here, we use Raman scattering to demonstrate experimentally that spin-phonon coupling is significant in RbCoCl_3 and has unusual characteristics. We employ a theoretical model that has been adapted from earlier work to determine the coupling strengths. We find indeed that the coupling is significant and is strong enough to warrant serious consideration in developing applications of interest vis-à-vis the physical properties of 1D ordered RbCoCl_3 .

Results

Experiment. The three vibrational modes of E_{2g} symmetry in RbCoCl_3 can be expected to be observed in (ZX) polarization along with the magnetic excitations^{6,13}. Although the original Raman study of RbCoCl_3 was a very general one¹³, the X(ZX)Y scattering geometry was selected for a detailed characterization of the magnetic excitations as a function of temperature. Under these experimental circumstances, only the E_{1g} mode and one of the E_{2g} modes at 132.1 cm^{-1} , which appears weakly in the X(ZX)Y spectrum via polarization leak-through arising from imperfect experimental conditions, have been studied in the detail required for an analysis of their spin-phonon coupling. The sample temperatures reported here, when compared with those reported in¹³, have been corrected for a laser heating of 8 K, which was determined from a preliminary analysis of the temperature dependences of the magnon peak parameters, where the supposed temperatures of T_{N1} and T_{N2} were found to be 20 K and 4 K, respectively, for the accepted temperature values of 28 K and 12 K, respectively.

A typical result obtained for measurements of the X(ZX)Y polarized Raman spectrum of RbCoCl_3 at low temperature and at lower frequency is shown in Fig. 2. The phonon peaks have been curve fitted with an anharmonic oscillator model to ascertain their mode frequency, damping, and strength (following Ref.¹³). It is seen that two of the phonon modes (the E_{1g} mode and an E_{2g} mode) occur in close proximity to magnon peaks, making them promising candidates for spin-phonon studies.

Theory. It is known that the magnetic behaviour of RbCoCl_3 can typically be represented by a spin Hamiltonian^{6,13} where the dominant term is

$$2J_1 \sum_j \left[\alpha \mathbf{S}_j \cdot \mathbf{S}_{j+1} + (1 - \alpha) S_j^z S_{j+1}^z \right]. \quad (1)$$

Here $J_1 > 0$ is the nearest-neighbour exchange interaction between spin vectors labelled as \mathbf{S}_j and \mathbf{S}_{j+1} along a chain of Co ions (see Fig. 1). There is a linear combination of Heisenberg and Ising terms, proportional to $\mathbf{S}_j \cdot \mathbf{S}_{j+1}$ and $S_j^z S_{j+1}^z$ respectively, where it has been estimated from neutron and Raman scattering data^{5,6} that $\alpha = 0.112$. The spin Hamiltonian also contains a similar term describing the anisotropic (Heisenberg plus Ising) exchange interaction J_2 to next-nearest neighbours along a chain. The role of the interchain exchange interaction J' , which is much weaker, is mainly in causing a discretization of the band of magnons⁶.

The basic mechanism for the spin-phonon interaction (following previous studies mainly on rutile-structure antiferromagnets^{21,22}) is that, if we consider a bilinear exchange term of the general form $2J[\alpha \mathbf{S}_1 \cdot \mathbf{S}_2 + (1 - \alpha) S_1^z S_2^z]$, the exchange J between the two sites labelled 1 and 2 depends on the instantaneous coordinates of those sites, as well as the coordinates of other sites (for the Rb and Cl ions in this case) because of

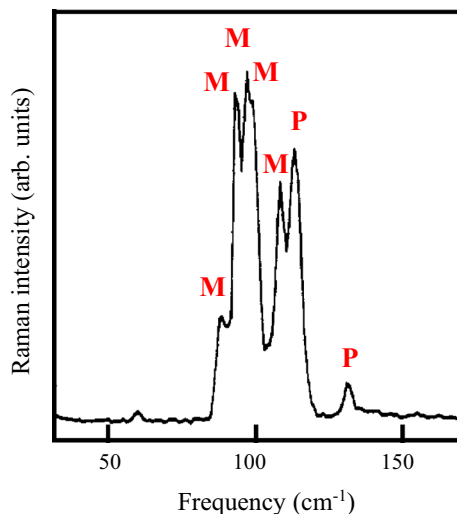


Figure 2. The low-frequency Raman spectrum of RbCoCl₃ recorded with a spectral resolution of 2.2 cm⁻¹ at ~ 11 K in X(ZX)Y polarization. The Raman peaks labelled M are magnetic excitations that have been evaluated elsewhere⁶, and those labelled P are the phonons of interest here.

super-exchange effects. When a Taylor series expansion about the equilibrium positions is made for this modulated exchange, there will be interaction terms that are linear in the displacements (and hence in the phonon amplitudes) and depend quadratically on the spins through the combination of terms appearing above. Thus, the renormalized frequency ω_{ph} of any phonon can be written in first order of perturbation theory as

$$\omega_{ph} = \omega_{ph}^0 + \lambda \langle \alpha \mathbf{S}_1 \cdot \mathbf{S}_2 + (1 - \alpha) S_1^z S_2^z \rangle, \quad (2)$$

where ω_{ph}^0 is the phonon frequency in the absence of spin–phonon coupling and λ is a constant (either positive or negative, depending on the phonon mode). The angular brackets around the spin products denote a statistical average involving the pairs of neighbouring spin sites. This quantity is approximately equal to $-S^2$ in the zero-temperature limit and its magnitude decreases monotonically with increasing T , becoming small (but nonzero) above T_{N1} . It is convenient to write the above frequency shift as

$$\Delta\omega_{ph} \equiv \omega_{ph} - \omega_{ph}^0 = -\lambda S^2 \Phi(T), \quad (3)$$

where we have introduced a pair correlation function by

$$\Phi(T) = -\frac{1}{S^2} \langle \alpha \mathbf{S}_1 \cdot \mathbf{S}_2 + (1 - \alpha) S_1^z S_2^z \rangle > 0. \quad (4)$$

This generalizes the definition given in our earlier work^{21,22} to the case where $\alpha \neq 1$, i.e., to include an Ising component to the bilinear exchange interaction. The numerical calculation for the T -dependence of $\Phi(T)$ may now be carried out following the method described previously, i.e., based on a modification of the so-called constant coupling approximation introduced in²³. The resulting estimate for RbCoCl₃ is shown in Fig. 3 (solid lines), taking account of the exchange coupling to the intrachain exchange interactions J_1 and J_2 . For comparison, the result for another Co compound, the rutile-structure antiferromagnet CoF₂, is also shown for temperatures above its T_N value. We note that the high-temperature ‘tail’ is quite small for RbCoCl₃ (being only ~ 10% or less of the low-temperature value for Φ). This is mainly due to the relatively large Ising component of the exchange in RbCoCl₃, as compared to the case of CoF₂.

Discussion

The main results are for the dependence of the phonon frequencies on temperature, as observed by Raman scattering and interpreted by the theory just described. Figures 4 and 5 show the frequencies plotted versus temperature for the E_{1g} mode and E_{2g} (132.1 cm⁻¹) mode, respectively. In both cases there is a clear and abrupt effect occurring in the measured data in the vicinity of the temperature T_{N1} , below which the 1D antiferromagnetic order sets in along the Co chains. To provide interpretation we have drawn some guide-to-the-eye lines in these figures. First, we note that the solid red line drawn through the data for $T < T_{N1}$ has just the behaviour displayed in Fig. 3 for the spin–spin correlation function $\Phi(T)$. The horizontal dashed red line provides an estimate for the $\Phi = 0$ base line representing the absence of spin–phonon coupling (after allowing for a high-temperature tail, as in Fig. 3). A comparison with Eq. (3) then allows us to deduce the spin–phonon coupling parameter λ for each phonon mode. We obtain the approximate values $\lambda S^2 = -1.8$ cm⁻¹ and -1.6 cm⁻¹ for the E_{1g} and E_{2g} phonons, respectively, which are of comparable magnitude to values previously found for rutile-structure antiferromagnets^{21,22}. In RbCoCl₃, however, there is an additional effect evident at T_{N1} . This is evident

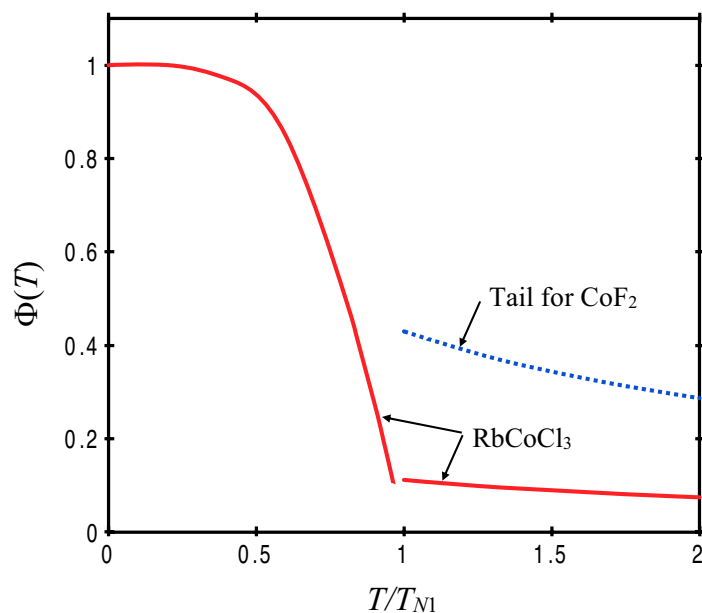


Figure 3. The T -dependence of $\Phi(T)$ estimated for RbCoCl_3 at temperatures T below and above T_{N1} . A comparison with CoF_2 at high temperatures is also shown.

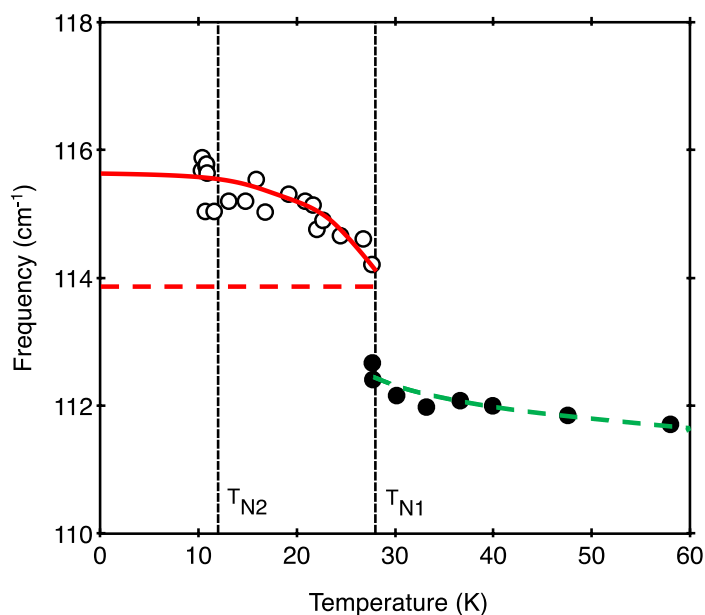


Figure 4. Temperature dependence of the E_{1g} mode frequency (data points) from Raman scattering measurements. The other lines are guides to the eye and are used in the theory (see the text).

on observing an unusual mismatch between the horizontal dashed red line below T_{N1} and the corresponding phonon frequency just above T_{N1} (as represented by the dashed green line). There is a “shift” (discontinuity) of about 1.8 cm^{-1} at T_{N1} for the E_{1g} mode, whereas for the E_{2g} mode the shift has the opposite sign and a magnitude of about 1.5 cm^{-1} .

The data shown in Figs. 4 and 5 therefore reveal that, in addition to a spin-phonon interaction in RbCoCl_3 , the quasi-1D ordering at T_{N1} induces a structural phase transition. The abrupt shift in phonon frequency of both the E_{1g} and E_{2g} modes indicates that the transition is first-order in nature. The relative shift in frequency at T_{N1} when the temperature is lowered is $+1.8 \text{ cm}^{-1}$ for the E_{1g} phonon and -1.5 cm^{-1} for the E_{2g} phonon. Given that the normal modes for the A_{1g} and E_{1g} modes²⁰ comprise Cl-ion motions perpendicular and parallel to the c axis, respectively, while the E_{2g} modes involve both Cl- and Rb-ion displacements within hexagonal planes, we conclude that the crystal lattice contracts a little along the c axis while expanding in the a - b plane when the

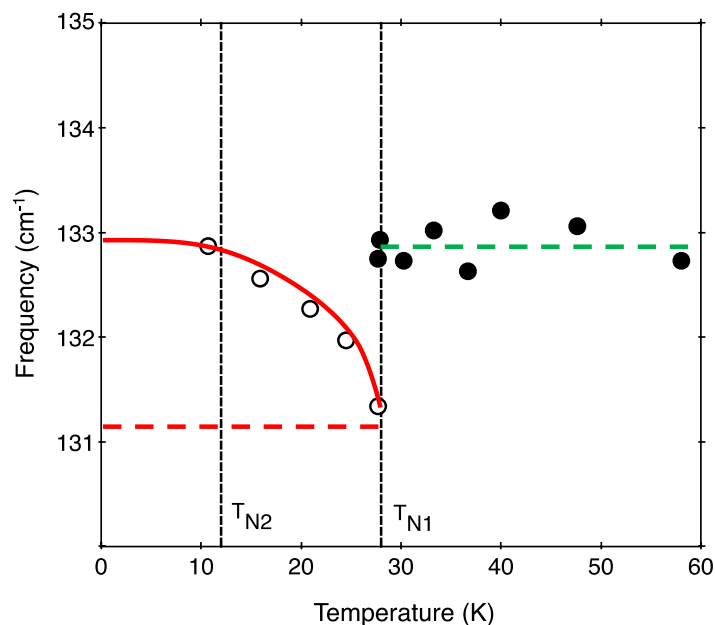


Figure 5. The same as in Fig. 4, but for the E_{2g} phonon mode frequency.

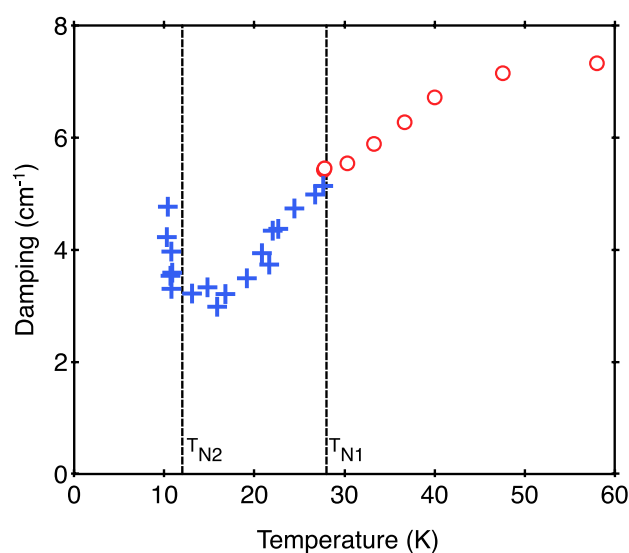


Figure 6. Temperature dependence of the E_{1g} mode line width from Raman scattering measurements.

temperature is lowered to T_{N1} and below. The lack of an observable mode splitting of the E_{2g} mode at T_{N1} and lower temperatures indicates that the crystal still has a hexagonal structure or has been lowered to that of a triclinic structure rather than a possible monoclinic structure.

Some further properties obtained for the E_{1g} phonon are shown in Figs. 6 and 7, where the mode damping and intensity, respectively, are plotted versus temperature. The E_{1g} phonon damping shows no anomaly at T_{N1} and continues to decrease smoothly with decreasing temperature, which is a normal behavior for a phonon in a nonmagnetic crystal in any case, but unexpectedly it then sharply increases below the 3D magnetic ordering temperature T_{N2} (see Fig. 6). The E_{1g} phonon Raman intensity exhibits an even more complicated variation with temperature (see Fig. 7). These characteristics would warrant further attention.

Conclusions

In conclusion, we have demonstrated unusual properties for the spin-phonon interactions in influencing the phonon frequencies for two modes in RbCoCl_3 with frequencies comparable to those of the low-frequency magnons. Our theoretical analysis, with modifications included to take account of the large Ising-like character demonstrated by the exchange interactions between spins, enabled the spin-phonon coupling coefficients to be deduced. This newly-observed aspect of the crystal properties at, and below T_{N1} , deserves further investigation

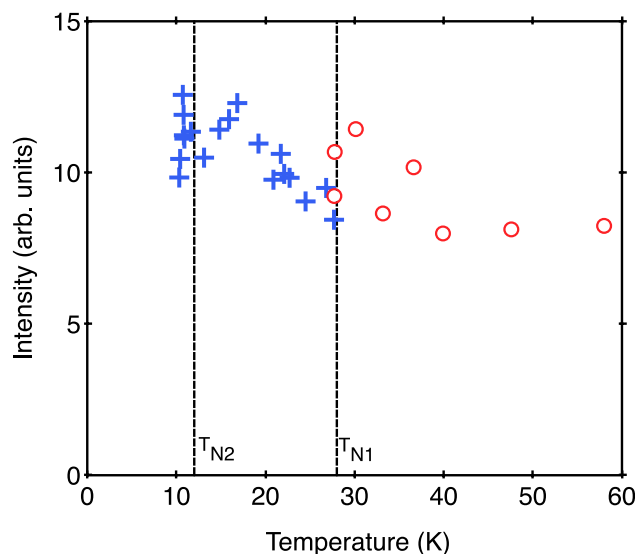


Figure 7. Temperature dependence of the E_{1g} mode intensity from Raman scattering measurements.

with high resolution x-ray diffraction and both inelastic and elastic neutron scattering. Such magnetic-ordering-related lowering of the crystal structure has been noted previously for CsCoBr_3 ²⁴, but nothing transpires as drastically at T_{N1} as that occurring in RbCoCl_3 .

Methods

The Raman measurements were performed on a single crystal of dark-blue colored RbCoCl_3 . The sample was mounted in a Thor S500 continuous-flow cryostat, where the crystal temperature could be controlled to within 0.1 K. The Raman scattering spectra were excited with 50 mW of 476.5 nm argon laser light, analyzed with a Spex 14018 double monochromator, and detected with a cooled RCA 31034A photomultiplier. The Raman signal was recorded at right angles to the incident light in a $X(\cdot)Y$ scattering geometry, where the Y axis was chosen to be normal to the crystal $(1\bar{1}20)$ cleavage plane and the Z axis was along the crystal c axis.

Data availability

All data generated or analysed during this study are included in this published article.

Received: 26 June 2022; Accepted: 4 August 2022

Published online: 18 August 2022

References

- Cottam, M. G. & Lockwood, D. J. *Light Scattering in Magnetic Solids* (Wiley, 1986).
- Lukaszew, R. A. (ed.) *Handbook of Nanomagnetism: Applications and Tools* (Jenny Stanford Publishing, 2016).
- Fermon, C. & Van de Vooorde, M. (eds) *Nanomagnetism: Applications and Perspectives* (Wiley, 2017).
- Rana, B., Mondal, A. K., Bandyopadhyay, S. & Barman, A. Applications of nanomagnets as dynamical systems—part I. *Nanotechnology* **33**, 062007 (2022).
- Hänni, N. P. *et al.* Magnetic order in the quasi-one-dimensional Ising system RbCoCl_3 . *Phys. Rev. B* **103**, 094424 (2021).
- Cottam, M. G. & Lockwood, D. J. Zeeman-ladder analysis of the Raman magnon energies in the quasi-one-dimensional antiferromagnet RbCoCl_3 . *Phys. Rev. B* **105**, 064411 (2022).
- Yoshizawa, H., Hirakawa, K., Satija, S. K. & Shirane, G. Dynamical correlation functions in a one-dimensional Ising-like antiferromagnetic CsCoCl_3 : A neutron scattering study. *Phys. Rev. B* **23**, 2298 (1981).
- Nagler, S. E., Buyers, W. J. L., Armstrong, R. L. & Briat, B. Ising-like spin-1/2 quasi-one-dimensional antiferromagnets: Spin-wave response in CsCoX_3 salts. *Phys. Rev. B* **27**, 1784 (1983).
- Lehmann, W., Breitung, W. & Weber, R. Raman scattering study of spin dynamics in the quasi-1D Ising antiferromagnets CsCoCl_3 and CsCoBr_3 . *J. Phys. C Solid State Phys.* **14**, 4655 (1981).
- Matsubara, F., Inawashiro, S. & Ohhara, H. On the magnetic Raman scattering in CsCoCl_3 , CsCoBr_3 , and RbCoCl_3 . *J. Phys. Condens. Matter* **3**, 1815 (1991).
- Goff, J. P., Tennant, D. A. & Nagler, S. E. Exchange mixing and soliton dynamics in the quantum spin chain CsCoCl_3 . *Phys. Rev. B* **52**, 15992 (1995).
- Nagler, S. E., Buyers, W. J. L., Armstrong, R. L. & Briat, B. Propagating domain walls in CsCoBr_3 . *Phys. Rev. Lett.* **49**, 590 (1982).
- Lockwood, D. J., Johnstone, I. W., Labbe, H. J. & Briat, B. Raman scattering from the 1D antiferromagnets RbCoCl_3 and RbNiCl_3 . *J. Phys. C Solid State Phys.* **16**, 6451 (1983).
- Lockwood, D. J. Magnon-phonon coupling in spin-1/2 quasi 1D antiferromagnets. In *Magnetic Excitations and Fluctuations* (eds Lovesey, S. W. *et al.*) 33 (Springer, 1984).
- Jörke, R. & Dürr, U. Properties of magnetic excitations in RbCoCl_3 . *J. Phys. C Solid State Phys.* **16**, L1129 (1983).
- Oosawa, A., Nishiwaki, Y., Kato, T. & Kakurai, K. Polarized neutron inelastic scattering study of anisotropic magnetic fluctuations in quasi-one-dimensional Ising-like antiferromagnet TlCoCl_3 . *J. Phys. Soc. Jpn.* **75**, 015002 (2006).
- Nagler, S. E., Buyers, W. J. L., Armstrong, R. L. & Briat, B. Solitons in the one-dimensional antiferromagnet CsCoBr_3 . *Phys. Rev. B* **28**, 3873 (1983).

18. Johnstone, I. W., Lockwood, D. J. & Dharmawardana, M. W. C. Influence of interchain coupling on the one-dimensional magnon Raman spectrum of CsCoBr₃. *Solid State Commun.* **36**, 593 (1980).
19. Lockwood, D. J. & Johnstone, I. W. Raman scattering from magnons and excitons in the 3-D ordered phases of CsCoBr₃. *J. Appl. Phys.* **53**, 8169 (1982).
20. Johnstone, I. W., Jones, G. D. & Lockwood, D. J. Anomalous phonon intensities in the Raman spectrum of disordered CsMg_{1-x}Co_xCl₃. *Solid State Commun.* **39**, 395 (1981).
21. Lockwood, D. J. & Cottam, M. G. The spin-phonon interaction in FeF₂ and MnF₂ studied by Raman spectroscopy. *J. Appl. Phys.* **64**, 5876 (1988).
22. Cottam, M. G. & Lockwood, D. J. Spin-phonon interaction in transition-metal difluoride antiferromagnets: Theory and experiment. *Low Temp. Phys. Fizika Nizkikh Temperatur* **45**, 90 (2019).
23. Elliott, R. J. Some properties of concentrated and dilute Heisenberg magnets with general spin. *J. Phys. Chem. Solids* **16**, 165 (1960).
24. Yelon, W. B., Cox, D. E. & Eibschutz, M. Magnetic ordering in CsCoBr₃. *Phys. Rev. B* **12**, 5007 (1975).

Acknowledgements

M.G.C. acknowledges support from the Natural Sciences and Engineering Research Council (NSERC) of Canada (grant RGPIN-2017-04429).

Author contributions

M.G.C. and D.J.L. initiated the work. D.J.L. performed the Raman scattering experiments and organized the data collection. M.G.C. developed the analytical theory and performed the analytical calculations. All authors contributed to the general discussion of the results and the writing of the manuscript.

Competing interests

The authors declare no competing interests.

Additional information

Correspondence and requests for materials should be addressed to M.G.C.

Reprints and permissions information is available at www.nature.com/reprints.

Publisher's note Springer Nature remains neutral with regard to jurisdictional claims in published maps and institutional affiliations.



Open Access This article is licensed under a Creative Commons Attribution 4.0 International License, which permits use, sharing, adaptation, distribution and reproduction in any medium or format, as long as you give appropriate credit to the original author(s) and the source, provide a link to the Creative Commons licence, and indicate if changes were made. The images or other third party material in this article are included in the article's Creative Commons licence, unless indicated otherwise in a credit line to the material. If material is not included in the article's Creative Commons licence and your intended use is not permitted by statutory regulation or exceeds the permitted use, you will need to obtain permission directly from the copyright holder. To view a copy of this licence, visit <http://creativecommons.org/licenses/by/4.0/>.

© The Author(s) 2022